Implementation of centralised, numerical busbar protection using distributed photonic current sensors

Philip Orr[a], Neil Gordon[a], Lloyd Clayburn[a], Zhuo Ma[a], Qiteng Hong[b], Dimitrios Tzelepis[b],

Nargis Shabbir Hurzuk[c], Rannveig Løken[c], and Campbell Booth[a,b]

[a]Synaptec Ltd, Glasgow, UK

[b]Institute for Energy and Environment, University of Strathclyde, Glasgow, UK

[c]Statnett SF, Oslo, Norway

philip.orr@synapt.ec

Abstract

Fast and robust busbar protection is critical to ensuring the reliability and safety of transmission substations and the connected power networks. For the most part, modern numerical busbar protection techniques remain based upon the interrogation of conventional current transformers (CTs) by copper secondary wiring feeding multiple IEDs ("peripheral units") which communicate measured currents to one or more central units using dedicated optical fibre digital communication links.

Numerical busbar protection requires copper secondary wiring in the yard that presents safety and cost challenges, particularly during substation refits. With the transition to digital substations, it becomes possible to collect all the measurements in sample value format from different bays on a common network (the process bus) without having dedicated wiring for each measurement, however there is a limited number of sample value streams that busbar protection IEDs available today can handle. Combining multiple active units into a single system and substantially eliminating copper wiring would lead to reductions in civil work, materials, outage times, and therefore to both capital and operational expenditure.

In this paper, we report on the design and testing of the first centralised busbar protection scheme that makes use of distributed photonic current sensors. By utilising distributed, passive sensors which are interrogated purely using standard optical fibre, the requirement for active units in the substation yard is completely eliminated. Additionally, the use of copper wiring from CTs to measurement units may be eliminated. The scheme, designed and built for Statnett by Synaptec, will be installed and trialled at Statnett's Furuset R&D substation near Oslo, Norway. A prototype centralised busbar protection algorithm, validated with the University of Strathclyde, will run on the central merger unit to prove the principle of centralised busbar protection using a single active IED.

The goal of developing and deploying the presented system is to enhance both redundancy and failure detection probability of busbar protection, and to enable the safe, continued operation of the busbar protection scheme during refurbishment projects for control systems. With further development, or following integration of the instrumentation platform with a conventional protection IED, it is proposed that this technique could be deployed in a business as usual context.

1 Introduction

Fast and robust busbar protection is critical to ensuring the reliability and safety of transmission substations and the connected power networks. Although having a relatively low probability of occurrence [1], failure to clear busbar faults in a timely manner has the potential to severely damage the entire substation, causing prolonged outages [2]. Moreover, when busbar faults occur, a greater part of the grid is disconnected leading to longer and more severe power outage and diminished availability and stability of the network.

For the most part, modern numerical busbar protection techniques remain based upon the interrogation of conventional current transformers (CTs) by copper secondary wiring feeding multiple IEDs ("peripheral units") which communicate measured currents to one or more central units using dedicated optical fibre digital communication links [3,4]. In general, this modern approach is a great improvement over conventional hard-wired protection. However, numerical busbar protection requires copper secondary wiring in the yard that presents safety and cost challenges, particularly during substation refits.

With the transition to digital substations, it becomes possible to collect all the measurements in sample value format from different bays on a common network (the process bus) without having dedicated wiring for each measurement. It is even more imperative to include more measurements in one common busbar protection IED due to the limited number of sample value streams a particular busbar protection IED available today can handle. Combining multiple active units into a single system and substantially eliminating copper wiring would lead to reductions in civil work, materials, outage times, and therefore to both capital and operational expenditure [5].

In this paper, we report on the design and testing of the first centralised busbar protection scheme that makes use of distributed photonic current sensors. By utilising distributed, passive sensors which are interrogated purely using standard optical fibre, the requirement for active units in the substation yard is completely eliminated. Additionally, the use of copper wiring from CTs to measurement units may be eliminated. The scheme, designed and built for Statnett by Synaptec with the collaboration of the University of Strathclyde, will be installed and trialled at Statnett's Furuset R&D substation near Oslo, Norway by Q4 2019.

2 Description of passive electrical sensing mechanism

2.1 Background (OVTs and OCTs)

Optical current transducers (OCTs) are now relatively well established and are developed by a range of manufacturers for their passive and highly accurate measurement of electrical current [6,7]. Presently, the most successful design is based on either spun or annealed optical fiber (to reduce shape-induced linear birefringence) that is coiled around the conductor or current path. The contour integral of the circulating magnetic field then yields a polarimetric or interferometric measurement of enclosed current based on the Faraday effect [8] that is immune to the influence of external or stray fields. Optical voltage transducers (OVTs) have also been developed, primarily based upon either the electro-optic (Pockels) effect or the piezoelectric effect [7,9].

Both established OCTs and OVTs rely on interferometric or polarimetric measurement techniques, and thus the distance from interrogator to a single measurement location cannot be greater than around 10 km. Additionally, as with conventional electrical transducers (CTs and VTs), it is not possible to discriminate between superimposed sensor responses, and thus serial multiplexing is not possible.

For these reasons, wide-area coverage, measurement over long distances, and high numbers of sensors are not presently achieved by optical current or voltage measurement schemes. It is therefore of interest whether a new technology can be utilised to develop wide-area sensor networks or efficient and safe sensor networks around a substation environment.

2.2 Passive, wavelength-encoded current and voltage measurement

Synaptec and the University of Strathclyde have developed a platform technology that allows standard single-mode fibre (conventionally used in digital telecommunication networks) to be utilised as a medium to serially-multiplex a high number of passive current or voltage sensors throughout a power network. In this section, a description of this core method is provided to enable the reader to understand the measurement mechanisms, benefits, and limitations of the technology.

A. Fiber Bragg gratings (FBGs)

Fiber Bragg gratings (FBGs) are periodic perturbations of the refractive index along a fiber core, having peak optical reflection at a specific wavelength, known as the Bragg wavelength [10], and a typical physical length of 5–10 mm. In sensor applications, their wavelength-encoding nature, coupled with their simple reflected spectra, means that FBGs are relatively easy to interrogate and multiplex, and are effectively immune to the problems of intensity fluctuations and attenuation [11]. For these reasons the FBG is now ubiquitous in the field of optical instrumentation [12].

Peak optical reflection from FBGs occurs at a wavelength λ equal to twice the grating period, i.e. at $\lambda/n = 2\Lambda$ where n is the fiber refractive index and Λ is the pitch of the grating. Thus, straining or compressing the fiber longitudinally at the location of the grating shifts up or down, respectively, the peak reflected wavelength. Illumination of the FBG by broadband light, and some form of peak wavelength detection and tracking, may therefore be employed to utilize the FBG as a strain sensor.

B. Passive measurement of voltage and current using FBGs

The authors have previously developed fiber-optic voltage and current point sensors, based on FBG technology, that have been applied successfully to power system plant diagnostics [13,14]. The complete optical sensor system has been shown to be capable of measuring dynamically changing signals and has been successfully used for detecting higher order voltage and current harmonics [15].

The transducer utilizes an FBG bonded to a multilayer piezoelectric stack, while the current sensor uses a small, high-bandwidth current transformer monitored by a dedicated voltage sensor as shown in Figure 1. In both cases an FBG peak wavelength shift can be calibrated in terms of voltage or current, while a temperature measurement can also be performed simultaneously using the same sensors to allow for active compensation of thermal sensitivity changes over a broad range of environmental temperatures.

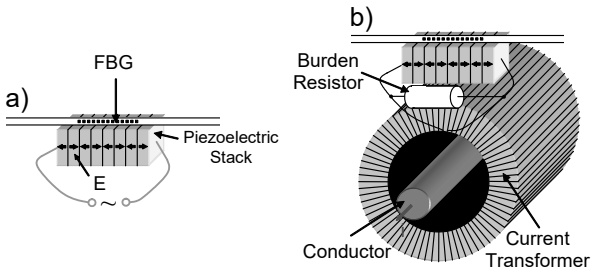

Figure 1. (a) Schematic of piezoelectric/photonic voltage transducer mechanism (b) Schematic of current sensor using CT and voltage sensing mechanism

It was demonstrated previously that these fiber-optic voltage and current sensors can be used for measuring variable frequency voltage and current waveforms for use in future aero-electric power systems [16].

2.3 Measurement of temperature, strain, and vibration

By removing the piezoelectric element from the mechanism described in the section above, it is possible to construct vibration, strain (quasistatic and dynamic) and temperature sensors which are compatible with the voltage and current sensors. In the proposed Furuset pilot, a selection of temperature and vibration sensors shall be included as part of the installation to demonstrate single-platform measurement of electrical and mechanical parameters. It is notable that this will be one of the first demonstrations of the use of Process Bus to convey temperature and strain information by customising the 61850-9-2 payload.

2.4 Central multi-point measurement acquisition and processing

The generic architecture of an FBG sensor scheme is illustrated in Figure 2. Light from an optical source is guided by fiber to an array of serially-multiplexed FBGs. Reflections from all FBGs are

returned via a coupler to the interrogating device, at which the peak reflected wavelength from each sensor is extracted.

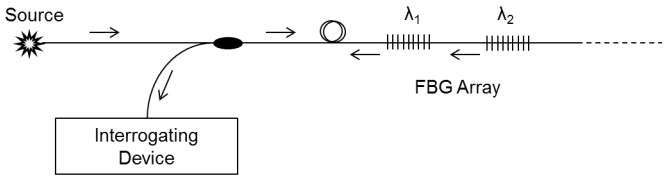

Figure 2. Schematic of general measurement topology illustrating the multiplexed and reflection-mode topology. λ1 and λ2 are peak reflected wavelengths.

The interrogating device can be thought of as a generalised implementation of a “merging unit”, or merger, interrogating multiple multiplexed sensors by illuminating them and continuously analysing the light reflected from each sensor. Figure 3 illustrates the general architecture of a current measurement scheme based on this platform, where the merger is deployed in a substation (having an available auxiliary power supply and time-synchronisation source) and the sensors are deployed in the field where no power or supporting infrastructure is available.

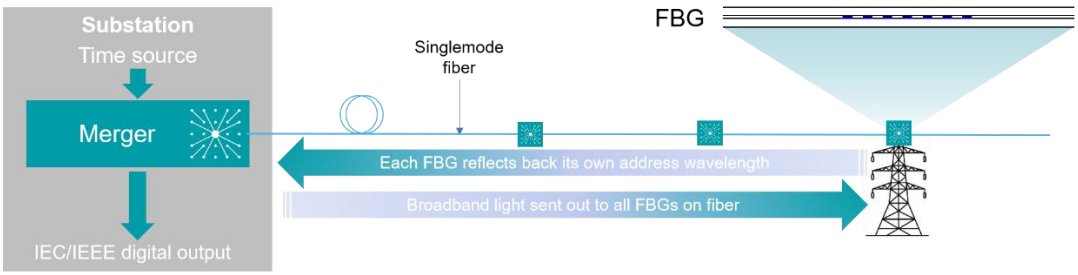

Figure 3. Example of current measurement topology on generic transmission line. A single merger is capable of measuring signals from 50 sensors over a maximum distance of 100 km.

The general architecture of the merger is set out in Figure 4. In the present deployment, a Xilinx Ultrascale 9EG is utilised as the core processing module, allowing functions to be deployed on an FPGA or real-time processor as appropriate. The system is based upon a broadband light source and receiving prism/CCD arrangement, with digital processing of the optical spectrum executed by the FPGA.

Voltage and current production and analysis, and the publishing of IEC 61850-9-2 Process Bus sampled values, are managed primarily by the real-time processor. Recent work in collaboration with the University of Strathclyde demonstrated the merger’s compliance with the IEC 61850-Cna9-2 standard [17].

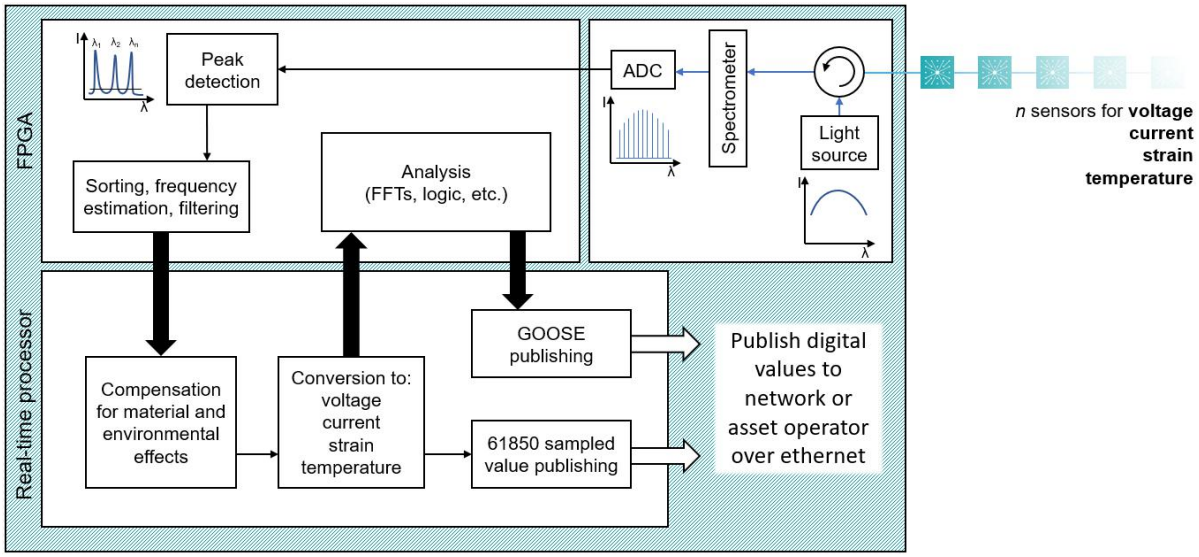

Figure 4. General architecture of merger.

The limitation of the present embodiment is interrogation of up to 50 sensors over a maximum distance of 100 km from the merger. This platform can be used for a variety of innovative applications on power networks to reduce costs by allowing protection and control systems to gather time-synchronised, accurate measurements cost-effectively over wide-areas or around digital substations. In the next section, we set out how the platform is being used to implement centralised instrumentation and protection for a transmission busbar at the Furuset digital substation in Oslo, Norway.

3 Design of centralised busbar instrumentation protection scheme

3.1 Traditional busbar protection systems

Busbar differential and circuit breaker failure protection is used as protection for all busbars in the solidly grounded system. Independent of system grounding, Statnett does not use double sets of busbar differential and/or circuit breaker failure protection. Figure 5 indicates the most commonly used forms of busbar protection.

A rail	BC rail	AB rail One breaker solution	AB rail Two breaker solution 1 current transformer	AB rail Two breaker solution 2 current transformers	AB rail with bypass	ABC rail
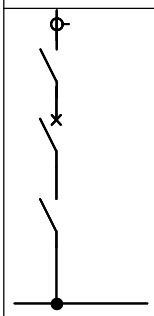	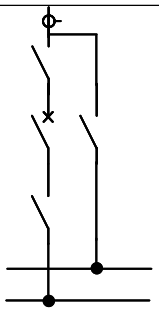	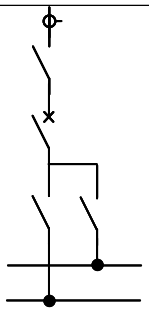	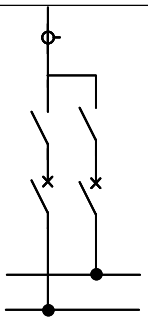	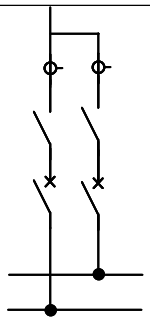	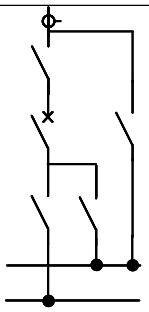	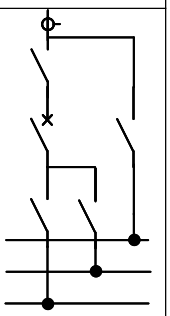

Figure 5. Common forms of traditional busbar protection

Busbar differential protection is generally of low impedance type, having separate current measurements for each phase, the functionality to protect two or more zones, selective disconnection of the fault in each zone, and using separate relay cores. The protection system must always release a three-phase definitive trip command to each trip-coil for each circuit breaker. The trip command from the busbar protection must not start any auto-reclose or synchronising sequences.

Depending on the busbar configuration and breaker positions, the busbar differential protection must include functionality for dynamic changes between protecting separate zones A and B or protecting one common zone for A and B. This dynamic change must depend on the breaker position signals connected to the busbar differential protection. Such dynamic changes must not cause any potential risk of unwanted action or blocking of the busbar protection. In addition, the sensitivity of the busbar differential protection must not be altered during such dynamic changes. In the case of this Furuset pilot installation, the breaker positions will not be taken into consideration, and hence the centralised busbar differential protection function shall initially be tested only on the basis of current measurement in all three phases of each bay.

3.2 Challenges for busbar protection in substations with Process Bus

In a Digital Substation Automation System (DSAS) based upon a Process Bus architecture, IEDs normally have some limitations in terms of the number of sampled value (SV) streams that can be handled; this limitation relating to the processing power and capability of the IEDs. From experience gained during the pilot project in Statnett based on the Process Bus, if a double breaker, double CT system is used, it can be challenging to implement a busbar protection system which must handle one SV stream from each CT connected to the protected busbar. For larger substations, this is likely to be a greater challenge.

A centralised busbar protection implementation based upon distributed photonic sensors will provide valuable experience in terms of handling current measurements from a large number of bays. In this pilot, the Synaptec merger with an onboard busbar protection algorithm shall operate as a parallel system to the existing busbar protection system from ABB based on analogue measurements, and will be a proof of concept of a multi-sensor-based protection scheme compared directly with traditional analogue measurements. The successfully implemented centralised scheme will also be relevant in the case of refurbishment projects, where it is required to have busbar protection in operation for the duration of the rebuild.

3.3 Centralised busbar protection scheme

Using the distributed measurement platform described in Section 2, multiple measurements of current may be deployed throughout a substation, serially linked only by standard single-mode optical fibre and interrogated from a single end. For a five-feeder busbar topology of the type under consideration at the Furuset substation, full unit protection functionality can be delivered by 15 distributed photonic current sensors. Since primary-connected conventional CTs are already present on each feeder, five three-phase secondary-connected current sensor units (SUs) are sufficient for full measurement coverage. Figure 6 shows a block diagram of the measurement topology, including additional mechanical sensors for condition monitoring of a transformer.

The merger system as described in Section 2 is housed in a standard 3U, 19-inch rack-mount enclosure and will be mounted in the protection and control rack of the Furuset substation relay room with access to a power supply and GPS time synchronisation via Precision Time Protocol (PTP). Single-mode optical fibre will connect the merger to each of the five sensor units in series. The sensor units are 2U, 19-inch rack-mount enclosures of customised design for integration within Statnett's existing bay cabinets, and each contains three secondary-connected current sensors for monitoring of the CT at each feeder location. As described in Section 2, each current sensor will convert the secondary quantity into an analogue optical measurement which is received by the merger, calibrated and output to the process bus in the IEC 61850-9-2 sampled value format. In parallel, the merger will perform the busbar protection algorithm using the calibrated current measurements and output trip

signals to the process bus in the IEC 61850 GOOSE protocol. Implementation and testing of the protection algorithm is outlined in Section 4.

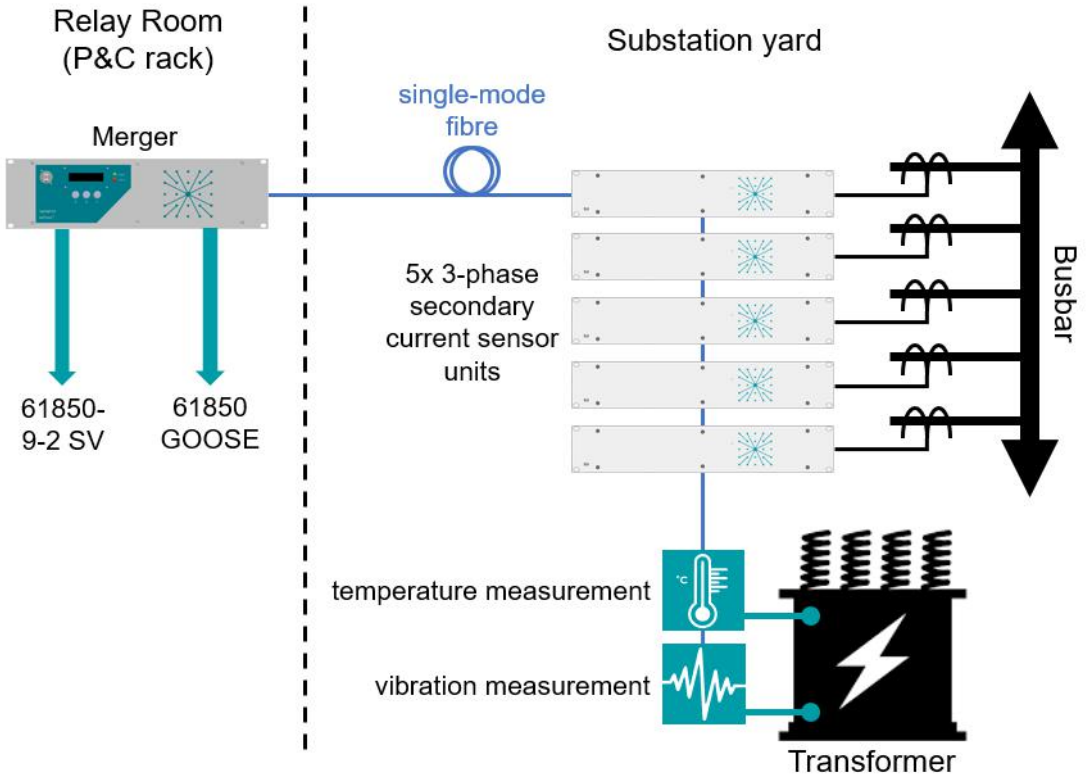

Figure 6. Block diagram of the Furuset busbar instrumentation protection scheme using distributed photonic current sensing.

The mechanical sensors will be spot-welded or epoxied onto the surfaces to be monitored, and optical measurements will also be calibrated by the merger and output as 61850-9-2 sampled values for visibility to the SCADA system.

4 Protection algorithm development and integration

4.1 Centralised busbar protection algorithm

For the purposes of testing the proposed centralised busbar protection based upon distributed photonic sensors, a generic biased differential protection algorithm has been developed in Matlab/Simulink.

A biased differential protection suggests that the operating current I_{OP} is continuously adjusted by the derivation of the differential current I_{diff} and biasing current I_{bias}. Biasing is applied to ensure stability of protection to external faults while permitting relative sensitive settings to pick up internal faults. The operating region of biased differential protection is depicted in Figure 7 and the operating current I_{OP} is formulated according to the following expression:

$$I_{OP} = \begin{cases} I_{s1}, \ for \ I_{bias} < I_{s2} \\ I_{s1} + K(I_{bias} - I_{s2}) \ for \ I_{bias} > I_{s2} \end{cases}$$

where:

I_{s1}:$Pick - up\ current$

I_{s2}:$Bias\ curernt\ threshold, above\ which\ the\ slope\ K\ is\ used.$

K:$Biasing\ slope$

I_{bias}:$Biasing\ current$

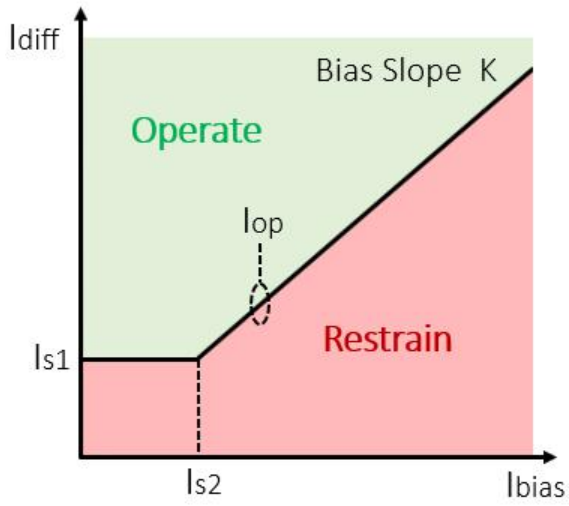

Figure 7: Differential protection biased characteristic.

The protection algorithm will initiate a tripping when the differential current is within the operating region (i.e. green-shaded area) otherwise will remain stable (i.e. red-shaded area).

4.2 Testing of centralised busbar protection algorithm

Strathclyde's multi-terminal model was modified to reflect a generic busbar topology representative of the busbar under consideration at the Furuset substation. The modified system under test comprised a busbar with five feeders in total. Two feeders had grounded synchronous generators at each end, two feeders had transmission line sections and parallel grounded RLC loads at each end, and one feeder had a transmission line section, parallel RLC load and grounded three-phase source. Each feeder had a three-phase current sensor measuring primary current located at the busbar terminal, representative of the measurement locations of the instrumentation topology to be deployed. Current transformers were omitted in the simulation. The simulation contained nodes for the measurement of fault currents, with faults programmed via MATLAB script at the busbar location or at any of the three transmission line sections. The topology of the model is shown in Figure 8.

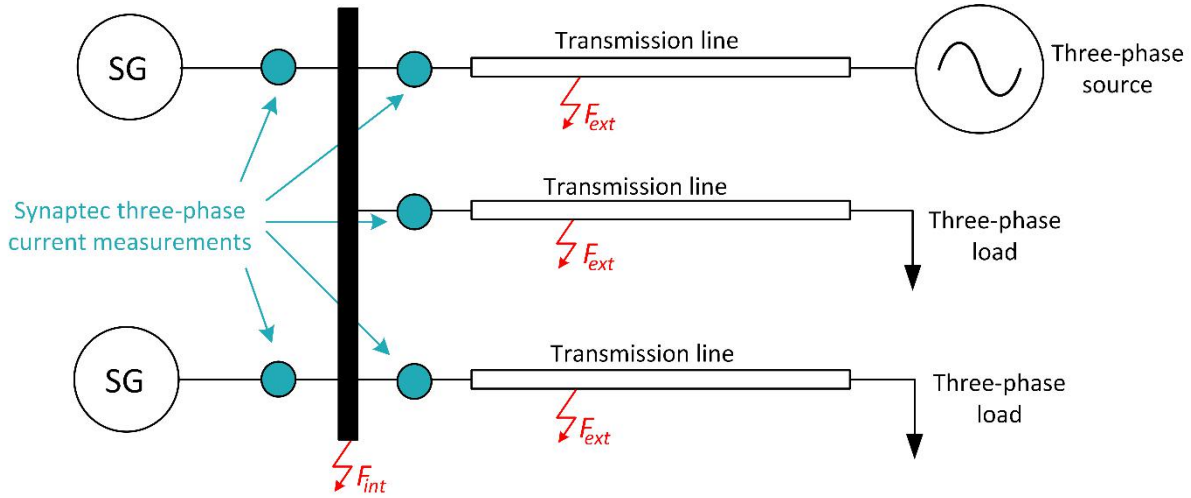

Figure 8: Network topology

The minimum fault condition was determined using a 100 Ω purely resistive fault at the busbar location. Differential protection settings were generated based on the minimum single phase and three phase fault current phasors obtained through simulation. Fault current phasor measurement was taken at an arbitrary point in time during the fault.

Differential protection was performed for each phase of the power system, using ordinary phasors rather than symmetrical components. In this simulation, the MATLAB FFT function was used to calculate phasors. Prior to application of the FFT, the signal was frequency redshifted by 18.75 Hz such that the 50 Hz component falls into the centre of a bin and thus spectral leakage is minimised. The FFT was length 256 samples; 240 samples measured at 4 kHz, padded with 16 zeros. The protection algorithm was re-implemented in Verilog and deployed on the central merger's FPGA.

The simulation was tested in Simulink for both external and internal faults (waveforms in Figure 9). The fault types considered were three-phase, three-phase to ground, solid three-phase, phase-to-phase, and phase-to-phase-to-ground. Example results are shown in Table 1 for a fault initiation time of 0.4s into simulation.

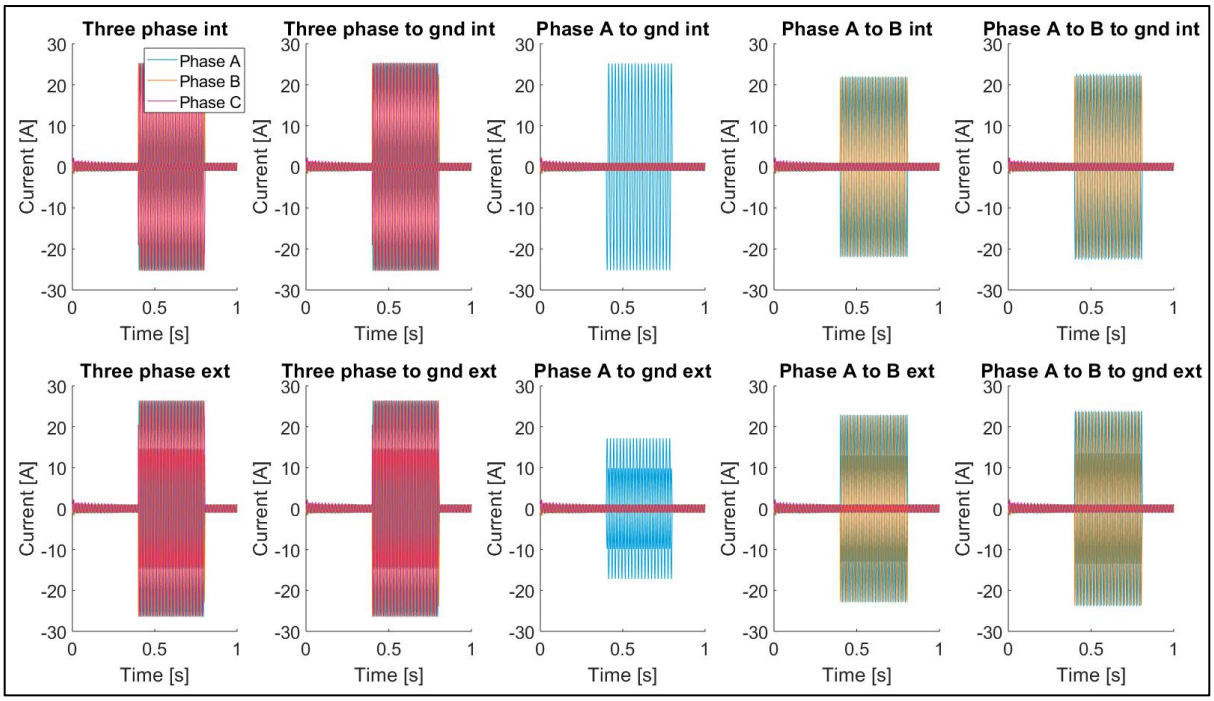

Figure 9: Fifteen currents (5 sensors x 3 phases) applied to Synaptec sensors in the FAT for a range of fault scenarios. Int: internal fault at busbar, Ext: external fault. The fault is applied at 0.4 s and cleared at 0.8 s.

Table 1: Algorithm trip times for each phase indexed by fault type

Fault type	Phase A trip [s]	Phase B trip[s]	Phase C trip [s]
Internal			
Three phase	0.413	0.411	0.411
Three phase to ground	0.413	0.411	0.411
Phase A to B to ground	0.412	0.413	NO Trip
Phase A to ground	0.413	NO Trip	NO Trip
Phase A to B	0.412	0.412	NO Trip
Solid three phase	0.403	0.400	0.400
External			
Three phase	NO Trip	NO Trip	NO Trip
Three phase to ground	NO Trip	NO Trip	NO Trip
Phase A to B to ground	NO Trip	NO Trip	NO Trip
Phase A to ground	NO Trip	NO Trip	NO Trip
Phase A to B	NO Trip	NO Trip	NO Trip
Solid three phase	NO Trip	NO Trip	NO Trip

4.3 Integration and testing of busbar protection algorithm on merger platform

The algorithm as tested in the prior section was re-implemented in Verilog for deployment on the merger's FPGA. The system is required to calculate one FFT per phase at a rate of 4 kHz, which is a significant processing burden for a distributed sensor system measuring 18 sensors. The FFTs were implemented in an efficient pipelining format, and the protection logic was also implemented on the FPGA following calculation of the 18 phasors.

In order to test the phasor production and protection logic, the merger was configured to accept synthesized input waveforms generated in the simulations in Section 4, bypassing the merger's sensor interrogation blocks. The merger platform was then verified against the simulation results in Table 1 to ensure it delivered the same results.

5 Injection testing of full system

The proposed centralised busbar protection scheme has been tested using secondary injection as illustrated in Figure 10. Three-phase instantaneous fault currents from internal and external faults simulated using the Simulink model shown in Figure 8 have been recorded as .mat files, which are subsequently converted to COMTRADE files for the injection tests. The COMTRADE files are then loaded to RTDS's PLAYBACK function block [18], which is used for playing back the signals that were recorded in the COMTRADE format. There are five feeders connected to the busbar in the network model, each with three-phase currents, so there are 15 current signals recorded. Due to the limitation of the amplifier output number, in the tests, one phase (i.e. Phase A) from each feeder has been selected for the tests, i.e. in total, five currents signals are amplified and injected to the merger. The recorded current signals are first scaled down to the range of ±10 V, which is the output range of the RTDS's analogue output card. The signals output from the RTDS are sent to the amplifiers, where they are amplified to currents with a nominal value of 1 A. The amplified currents are then injected to the sensors, which perform the measurement (e.g. current, temperature, vibration, etc.) and send them to the merger. The merger will conduct the analysis of the measured currents from the five sensors using the proposed centralised busbar protection algorithm. The merger can also output the measurements in IEC 61850 Sampled Value (SV) format [19], which can be used for monitoring purpose using a PC. The tripping signal from the merger is sent using IEC 61850 GOOSE messaging [20] and recorded in RTDS. By comparing the time of the fault and the time when a tripping signal is received at RTDS, the total tripping time (excluding the circuit breaker operating time) can be determined.

The test results for an internal three-phase fault at the busbar are shown in Figure 10. The first five plots show the instantaneous current measurements from Phase A of the five measurement points, while the last plot shows the tripping signal for Phase A. It can be seen that the fault occurs at 3.527s and the tripping signal is received via GOOSE at 3.545s, where the total tripping time is approximately 18 ms. Different internal and external faults were applied and Table 1 presents the summary of the test results.

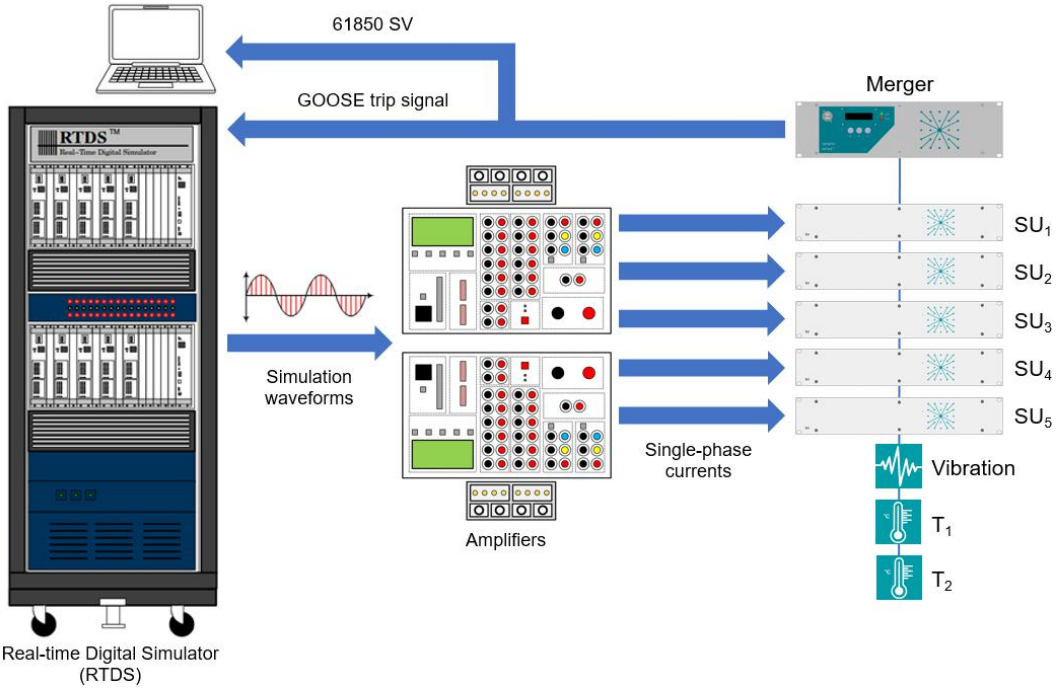

Figure 10. Test setup for validating the proposed scheme using secondary injection

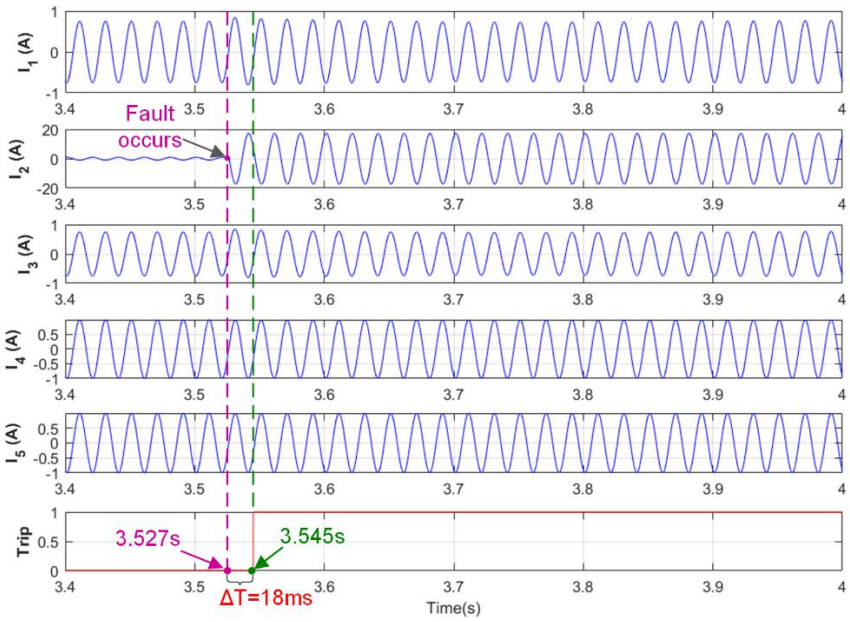

Figure 11. Test results for an internal three-phase fault at the busbar

6 Conclusions

In this paper we have reported on the design and testing of the first centralised busbar protection scheme that makes use of distributed photonic current sensors. By utilising distributed, passive sensors which are interrogated purely using standard optical fibre, the requirement for active units in the substation yard was completely eliminated. Additionally, the use of copper wiring from CTs to measurement units may be eliminated. The scheme, designed and built for Statnett by Synaptec, will be installed and trialled at Statnett's Furuset R&D substation near Oslo, Norway. A prototype centralised busbar protection algorithm, validated with the University of Strathclyde, will run on the central merger unit to prove the principle of centralised busbar protection using a single active IED.

The goal of developing and deploying the presented system is to enhance both redundancy and failure detection probability of busbar protection, and to enable the safe, continued operation of the busbar protection scheme during refurbishment projects for control systems. With further development, or following integration of the instrumentation platform with a conventional protection IED, it is proposed that this technique could be deployed in a business as usual context.

References

[1] Guide for Protective Relay Applications to Power System Buses, IEEE Standard C37.234, 2009

[2] K. M. Silva, A. M. P. Escudero, F. V. Lopes and F. B. Costa, "A Wavelet-Based Busbar Differential Protection," in IEEE Transactions on Power Delivery, vol. 33, no. 3, pp. 1194-1203, June 2018.

[3] G. Ziegler, "Numerical Differential Protection: Principles and Applications", 2en ed. Berlin, Germany, 2012

[4] Alstom Grid, "Network Protection & Automation Guide", May 2011

[5] P. Orr et al., "Distributed Photonic Instrumentation for Power System Protection and Control," in IEEE Transactions on Instrumentation and Measurement, vol. 64, no. 1, pp. 19-26, Jan. 2015.

[6] Alstom NXT Phase COSI Products, http://www.nxtphase.com (Accessed 24/01/2012)

[7] K. Bonhert, P. Gabus, J. Kostovic, H. Brandle, “Optical fiber sensors for the electric power industry,” Optics and Lasers in Engineering (Elsevier), vol. 43, pp. 511–526, 2005.

[8] Y. N. Ning, Z. P. Wang, A. W. Palmer, K. T. V. Grattan, and D. A. Jackson, “Recent progress in optical current sensing techniques,” Rev. Sci. Instrum., vol. 66, no. 5, pp. 3097-3111, 1995.

[9] Pan, F., Xiao, X., Xu, Y., and Ren, S., “An Optical AC Voltage Sensor Based on the Transverse Pockels Effect,” Sensors (Basel) 11(7), 6593–6602 (2011)

[10] G. Meltz, W. W. Morey, W. H. Glenn, “Formation of Bragg gratings in optical fibers by a transverse holographic method,” Opt. Let., vol. 14, no. 15, pp. 823–825, August 1989

[11] P. Niewczas, J. R. McDonald, “Advanced optical sensors for power and energy systems,” IEEE Instrumentation and Measurement Magazine, vol. 10, no. 1, pp. 18–28, February 2007

[12] A. Mendez, “Fiber Bragg grating sensors: a market overview,” Proc. SPIE, vol. 6619, p. 661905, 2007.

[13] L. Dziuda, P. Niewczas, G. Fusiek, J. R. McDonald, “Hybrid Fiber-Optic Voltage Sensor for Remote Monitoring of Electrical submersible Pump Motors”, Optical Engineering, Vol. 44, No. 6, pp 64401-1-6, June 2005

[14] L. Dziuda, G. Fusiek, P. Niewczas, G. Burt, and J.R. McDonald, “Laboratory Evaluation of the Hybrid Fiber-Optic Current Sensor”, Sensors and Actuators, A: Physical, Vol. 136, No. 1, pp. 184-190, May 1, 2007

[15] P. Niewczas, G. Fusiek, J. R. McDonald, “Dynamic capabilities of the hybrid fiber-optic voltage and current sensors”, IEEE Sensors Conference, Daegu, Korea, Oct. 22-25, 2006

[16] G. Fusiek, P. Niewczas, J. R. McDonald, “Concept Level Evaluation of the Optical Voltage and Current Sensors and an Arrayed Waveguide Grating for Aero-Electrical Systems’ Applications”, the 24th IEEE IMTC 2007 Instrumentation and Measurement Technology Conference, Warsaw, Poland

[17] Blair, S.M. and Burt, G.M. and Gordon, N. and Orr, P., “Wide area protection and fault location: review and evaluation of PMU-based methods”, 14th International Conference on Developments in Power System Protection (DPSP), March 2018

[18] RTDS Technologies Inc. , "User Manual - COMTRADE PLAYBACK", Dec 2012.

[19] International Electrotechnical Commission, "IEC 61850 9-2 Specific communication service mapping (SCSM) — Sampled values over ISO/IEC 8802-3", Dec 2011

[20] International Electrotechnical Commission, " Part 8-1: Specific communication service mapping (SCSM) – Mappings to MMS (ISO 9506-1 and ISO 9506-2) and to ISO/IEC 8802-3", Sep 2011